

---

# Evaluating histopathology transfer learning with ChampKit

---

**Jakub R. Kaczmarzyk**

Department of Biomedical Informatics  
Stony Brook Medicine  
jakub.kaczmarzyk@stonybrookmedicine.edu

**Tahsin M. Kurc**

Department of Biomedical Informatics  
Stony Brook Medicine  
tkurc@stonybrookmedicine.edu

**Shahira Abousamra**

Department of Computer Science  
Stony Brook University  
sabousamra@cs.stonybrook.edu

**Rajarsi Gupta**

Department of Biomedical Informatics  
Stony Brook Medicine  
rajarsi.gupta@stonybrookmedicine.edu

**Joel H. Saltz \***

Department of Biomedical Informatics  
Stony Brook Medicine  
joel.saltz@stonybrookmedicine.edu

**Peter K. Koo \***

Simons Center for Quantitative Biology  
Cold Spring Harbor Laboratory  
koo@cshl.edu

## Abstract

Histopathology remains the gold standard for diagnosis of various cancers. Recent advances in computer vision, specifically deep learning, have facilitated the analysis of histopathology images for various tasks, including immune cell detection and microsatellite instability classification. The state-of-the-art for each task often employs base architectures that have been pretrained for image classification on ImageNet. The standard approach to develop classifiers in histopathology tends to focus narrowly on optimizing models for a single task, not considering the aspects of modeling innovations that improve generalization across tasks. Here we present *ChampKit* (Comprehensive Histopathology Assessment of Model Predictions toolKit): an extensible, fully reproducible benchmarking toolkit that consists of a broad collection of patch-level image classification tasks across different cancers. ChampKit enables a way to systematically document the performance impact of proposed improvements in models and methodology. ChampKit source code and data are freely accessible at <https://github.com/kaczmarj/champkit>.

## 1 Introduction

Histopathology is the gold standard for diagnosing many types of cancers. There have been many efforts to apply computer vision techniques to histopathology throughout the years and it has gained more popularity with the emergence of deep learning [3–10]. There are many biologically and clinically important features that deep learning has been used to predict, including presence of invasive tumors [11–16], presence of tumor infiltrating lymphocytes [17–23], and prediction of microsatellite instability [24–28].

Whole-slide histopathology images are large (e.g., 100,000 by 100,000 pixels) relative to images used in standard deep learning applications like ImageNet [29]. In practice, they are processed into

---

\*Co-supervisors.

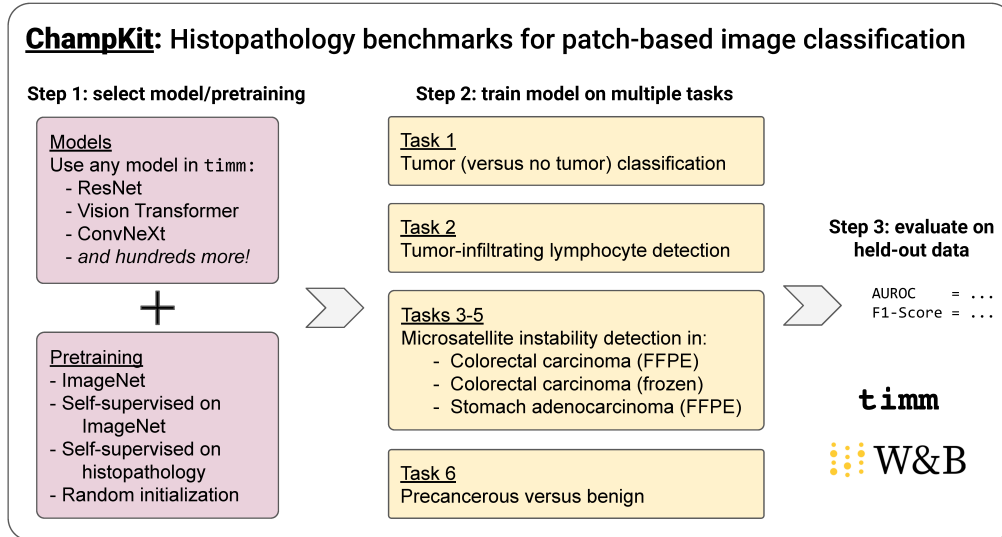


Figure 1: Overview of ChampKit. ChampKit enables systematic comparisons of model architectures and transfer learning across several patch-based image classification datasets. First, users select a model and pretrained weights from those available in timm [1] or a custom model with specification of pretrained weights or random initialization. Second, the models are trained on multiple tasks using identical training hyperparameters. Third, the trained models are evaluated on held-out test data for each task. Performance is tracked with Weights and Biases (W&B) [2].

smaller patches for use in machine learning. While most data processing and modeling happens at the patch-level, the overall prediction task falls either into patch-level classification or whole-slide (i.e. patient-level) classification. Whole-slide classification is used to predict a single label based on multiple image patches (e.g., response to cancer treatment, time to death, presence of somatic mutation). By contrast, patch-level classification aims to classify local features within individual patches, each of which has a label (e.g., detection of prognostic biomarkers and cancer cells). Whole-slide classification requires a different modeling approach, such as multiple-instance learning, whereas patch-level classification extends more naturally to traditional computer vision models, where each image is treated independently. Here we focus on patch-level image classification tasks.

Deep learning models for patch-level classification tasks tend to employ pretraining on ImageNet [17, 18, 24, 30–32], despite the fact that the original features are natural images. Recently, there has been growing interest in leveraging the success of self-supervised pretraining to directly learn features from unlabeled histopathology datasets [33, 34]. Many claims of performance improvements originate from studies where multiple deep learning architectures and/or (pre)training schemes are evaluated on a single dataset [17, 18, 35–37]. This is helpful to identify the modeling choices that are beneficial for the given dataset, but it does not inform whether the modeling innovations would generalize across different datasets and/or classification tasks.

To address this gap, here we introduce ChampKit (Comprehensive Histopathology Assessment of Model Predictions toolKit). ChampKit enables systematic and reproducible comparisons of model architectures and transfer learning across several patch-based image classification datasets. ChampKit provides easy access to a large collection of models and networks from timm [1]. ChampKit facilitates transfer learning/fine-tuning of those models for multiple patch-level classification tasks. The current implementation supports six diverse classification tasks across various cancers through publicly available datasets. ChampKit is extensible and allows integration with other custom models and datasets for benchmarking and comparison purposes. **ChampKit can greatly advance our ability to systematically identify the modeling innovations that generalize across patch-level histopathology classification tasks.**

## 2 Related work

**Model repositories.** A large number of deep neural networks are available in popular model repositories [1, 38–41]. These make it easy to employ models pretrained on ImageNet for image classification or for transfer learning for other tasks. One such repository, `timm` [1], provides hundreds of image classification models implemented in PyTorch [38] — with many models pretrained on ImageNet-1K or -22k — and training scripts for reproducibility. ResNet-based models are a popular choice for patch-level classification tasks in histopathology [18, 24, 30–32], while vision transformers have emerged as a candidate in recent studies [31, 42–44].

**Comparative studies of models in histopathology.** Laleh et al. [45] present benchmarks of many models for several multiple-instance-learning tasks, including patient-level survival prediction. These predictions are based on slide-level predictions, which are not directly comparable with patch-level classification tasks. Sharmay et al. [30] evaluate transfer learning in nine CNNs on two datasets. The nine CNNs are limited to variations of ResNets [46], DenseNets [47], and EfficientNets [48], and of the two datasets, one is not publicly available and the other is Camelyon [49], which is included in our benchmarks (task 1). Deining et al. [44] compare a vision transformer (DeiT [50]) to ResNet18 on two public datasets (a colorectal tissue classification dataset [51] and Camelyon). All of the models achieve accuracies greater than 0.998 area under the precision-recall curve on the colorectal cancer dataset, which suggests that it is not a meaningful dataset for model comparisons (We reproduced the near-perfect performance and therefore decided to exclude that dataset from the current report). The other datasets in their study are not publicly available. Kassani et al. [32] evaluate ensembles of CNNs (i.e., VGG19 [52], MobileNet [53], and DenseNet [47]). All four datasets are broadly based on benign versus malignant tissue classification, and a code repository is not provided in the paper. Springenberg et al. [31] provide an evaluation of several CNNs and vision transformers across five tasks, two of which are included in this study. Although their study is comprehensive, it does not include an evaluation of transfer learning, which is a common practice in histopathology analysis [17, 18, 24, 30–32].

In contrast to the studies above, we have curated a set of six diverse datasets for patch-level classification tasks that are publicly available. In addition, our benchmarking toolkit enables the evaluation of hundreds of different models, available in `timm`, including models pretrained on ImageNet-1K and -22K [29]. All of this is contained within a user friendly benchmarking toolkit that enables highly reproducible analyses, with extensions to custom models and datasets.

## 3 ChampKit

ChampKit is a one-stop-shop benchmarking toolkit that enables a systematic exploration of generalization performance of modeling choices and transfer learning across six patch-level histopathology classification tasks. ChampKit integrates the `timm` [1] model repository to provide access to hundreds of (pretrained) deep learning models, enabling evaluation across different transfer learning schemes from ImageNet [29] or from self-supervision on histopathology images [33, 54] or training the models from scratch. The datasets for each task are curated from different studies [55–59] and were selected based on diversity of the tasks and their importance for the biomedical community. Importantly, ChampKit provides insights into the modeling choices that are generalizable across patch-level classification tasks (not optimizing on a single dataset).

**Workflow.** After one chooses a model and pretrained weights (if any), the model is systematically trained on all six tasks (one model for each task). ChampKit includes scripts to perform an end-to-end analysis: download the models, prepare the datasets, train the models, and evaluate them on held-out test data. Weights and Biases [2] is used for logging experiment parameters and visualizing results across multiple models and training configurations.

**Custom models.** In addition to the popular (pretrained) computer vision models included in PyTorch, `timm` provides access to a much larger selection of models that have been pretrained on different datasets (e.g. ImageNet-1K and ImageNet-22K, and self-supervised pretraining on ImageNet-22K). Nevertheless, it may be desirable to tweak an existing model or employ a custom model. To include a custom model to ChampKit, a PyTorch [38] implementation of the model is required, as well as configuration options (i.e., input image size, location of pretrained weights if

they exist, and mean and standard deviation of input normalization). The ChampKit code repository includes an example of adding custom pretrained weights for a ResNet18 model [54].

**Custom datasets.** Beyond the six benchmark datasets, ChampKit allows for integration with custom datasets that are framed as a single-task patch-level (binary or multi-class) classification. Custom datasets must be organized in an ImageNet-like directory structure, in which the top-level directory contains directories `train`, `val`, and `test`, and each of those contains sub-directories of the different classes (e.g., `tumor-positive`, `tumor-negative`), where the corresponding patch-level images are located. Images can be of any size and will be resized during training and evaluation – the size is configurable.

## 4 Experiments

Using ChampKit, we provide strong baselines for each benchmark task using two models commonly used in histopathology, namely ResNet18 and ResNet50 [46], and a hybrid vision transformer (R26-ViT) [60] that has shown promise at image classification in smaller data regimes, which is similar in spirit to the patch-level analysis, but has not been widely applied to histopathology. The scope of this study is to demonstrate the utility of ChampKit and provide benchmarking baselines on a variety of datasets and models. We do not seek to make claims of state-of-the-art in any task or provide practice recommendations. ChampKit is a powerful benchmarking toolkit that enables a systematic analyses of many models across diverse datasets and could be used for this purpose in future work.

All models included comparisons of transfer learning from image classification on ImageNet-1K [29] and training from random weight initialization. ResNet18 comparisons also included transfer learning from a model trained using self-supervision on histopathology data [33, 54]. All models were implemented in `timm` using PyTorch, and pretrained ImageNet weights were accessed via `timm`, while the weights from self-supervised pre-training for ResNet18 were downloaded from [54].

All models were trained systematically using similar training hyperparameters in order to make fair comparisons across models and datasets. Models were trained to minimize the cross-entropy loss using the AdamW optimizer [61]. The learning rate was initially  $1e-6$  and warmed up to  $1e-4$  over the first three epochs, followed by a cosine schedule to a minimum value of  $1e-6$ , set for 500 epochs. All models employed a dropout rate of 0.3, DropPath [62] rate of 0.3, minibatch size of 84, label smoothing [63] of 0.1, and early stopping with a patience of 20 epochs based on validation loss. Automatic mixed precision was used via PyTorch’s [38] native implementation. Weights and Biases [2] was employed to log experiment parameters and to track training and validation metrics.

In addition, data was augmented using the RandAugment strategy [64] (magnitude 9, standard deviation 0.5), random cropping (to at most 95% of the image), and random erasing [65] (with a probability of 0.2 that a rectangle with an area between 1/50th and 1/3rd of the original image will be replaced with values sampled from a standard normal distribution). RGB channels were normalized with means (0.485, 0.456, 0.406) and standard deviations (0.229, 0.224, 0.225); these values are the means and standard deviations of the ImageNet training set. When using the R26-ViT or self-supervised ResNet18, images were normalized with means and standard deviations of (0.5, 0.5, 0.5) to match the normalization used in the pretraining. Images were resized to 224x224 with bicubic interpolation for R26-ViT and ResNet50, and bilinear interpolation for ResNet18.

Evaluation was done with model weights at 32-bit float precision based on early stopping. Area under the receiver operating characteristic curve (AUROC) and F1-score (threshold=0.5) were calculated (using `torchmetrics` [66]). Each experiment was run on a single NVIDIA Quadro RTX 8000 GPU with 48GB of video memory. A complete list of software versions can be found in the code repository.

## 5 Benchmark tasks and results

The benchmark datasets include six patch-based image classification tasks for: (1) tumor (versus no tumor) classification, (2) tumor-infiltrating lymphocyte detection, (3–5) microsatellite instability detection across different cancers and/or preparations, and (6) precancerous versus benign classification. ChampKit includes reproducible scripts to download all datasets, with the exception of the MHIST dataset [59], which requires completing an online form (an automated email is then sent

with a download URL). Details of each task are described alongside the results in the following subsections.

### 5.1 Task 1: tumor (versus no tumor) classification

Detection of tumor cells is critical in clinical histopathology. Tumor cells can have varied appearances and can be challenging to detect. In particular, small nests of tumor cells (<100 cells) might be difficult to detect, and this is one case where automated deep learning algorithms can be highly useful. This is especially true in sentinel lymph node biopsies, which are performed to determine whether cells from the primary tumor have metastasized. False negatives are unacceptable in this situation, and so deep learning methods for this task must be rigorously evaluated. Deep learning methods for tumor detection can also improve tumor detection sensitivity and potentially reduce false negatives [67]. We have included tumor detection as task 1 in our benchmark because of its clinical importance [68] and already wide-spread application in deep learning.

**Dataset.** The PatchCamelyon dataset [58] is a processed and curated version of the Camelyon16 dataset [49], containing 327,680 tumor and non-tumor images at  $96 \times 96$  pixels (10x magnification) from sentinel lymph node biopsies of breast cancer (Figure 2, Table 5 in Appendix). An image is positively labeled if the center  $32 \times 32$  pixel region contains at least one pixel of tumor. The PatchCamelyon dataset is licensed under Creative Commons Zero v1.0 Universal and is anonymized. PatchCamelyon is available for download [69] via Zenodo.

**Results.** For task 1, most models performed well according to AUROC and had more varied F1 scores (Table 1). Since false negatives is an unwanted outcome for tumor classification, the F1 score is a more relevant metric. Interestingly, pretraining consistently led to higher performance than training from randomly initialized weights. For ResNet18, self-supervised pretraining on histopathology improved performance over ImageNet pretraining, consistent with findings in [30]. Nevertheless, the R26-ViT architecture provides a strong inductive bias for this dataset (even without pretraining), performing as well as the best ResNet18 model with transfer learning; R26-ViT with pretraining yielded the best overall performance.

### 5.2 Task 2: tumor-infiltrating lymphocyte detection

Tumor-infiltrating lymphocytes (TILs) are clinically useful as prognostic biomarkers, related to the degree of immune response against a cancer. TIL quantification is important for predicting survival outcomes and guiding treatment decisions [70–73]. TILs tend to be 8-12  $\mu\text{m}$  in diameter with a dark, ovoid nucleus and scant cytoplasm [74]. Despite the subtle qualitative differences of TILs

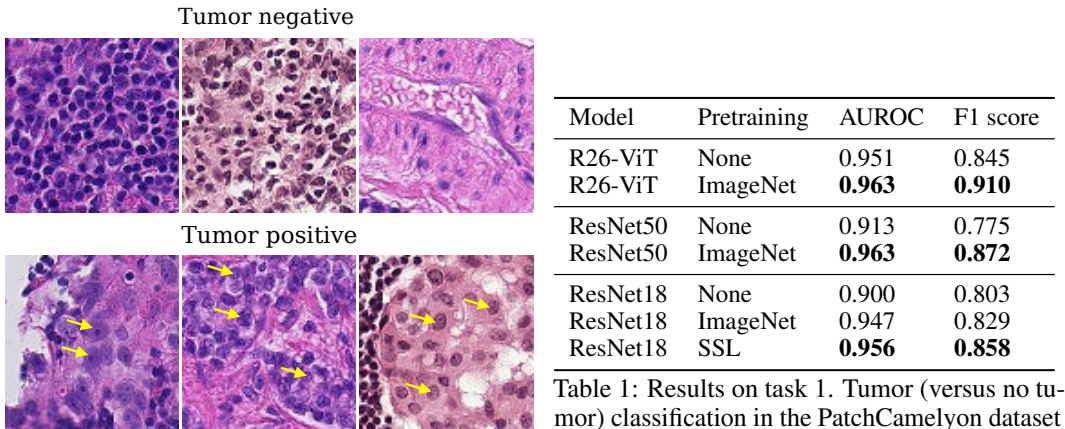


Figure 2: Sample tumor negative and tumor positive images from PatchCamelyon dataset [58]. The yellow arrows point to examples of tumor cells.

across image patches, pathologists can identify TILs through visual inspection. However, in practice, they tend to characterize only a small number of microscopic fields of view [68]. More detailed prognostic patterns can be made by mapping TILs at a whole-slide-level [75]. Thus, it would be greatly beneficial to clinicians to identify the patches that contain TILs across histopathology slides [17, 18, 72, 76]. Deep learning has the potential to address major drawbacks of manual TIL scoring: inter-observer variability and the scalability of TIL detection. In response, there has been much interest in applying deep neural networks to this task [17–19, 71, 77, 78]. Thus, task 2 consists of pan-cancer TIL detection because of its tremendous clinical relevance and popularity in deep learning.

**Dataset.** Task 2 dataset consists of 304,097 TIL-positive and TIL-negative images from [55], a curated subset of the data presented in [17, 18] (Figure 3, Table 5 in Appendix). This dataset includes 23 different cancer types from The Cancer Genome Atlas (TCGA) [79], representing a wide distribution of tissue types and stain differences. Patches are from formalin-fixed, paraffin-embedded (FFPE) whole slide images. Images are  $100 \times 100$  pixels at  $0.5 \mu\text{m}/\text{pixel}$  and are positive if they contain at least two TILs. No stain normalization was applied to the images. The data is licensed under Creative Commons Attribution 4.0 International. Images are anonymized, and there is no overlap in TCGA participants across data splits. This dataset is available for download via Zenodo [55].

**Results.** In general, all of the models do well at task 2, suggesting that there is strong predictive signal in the dataset (Table 2). In contrast to task 1, the ResNet18 architecture is best overall on this TIL detection task, even without pretraining. This agrees with [30], which reports that smaller models tend to perform better on some histopathology tasks. Pretraining with ImageNet and self-supervised learning provide an additional performance gain. However, in contrast to the findings in [30], self-supervised pretraining did not outperform ImageNet pretraining. Interestingly, training from randomly initialized weights outperformed transfer learning for R26-ViT. This is consistent with the findings of Kornblith et al. [80] and Raghu et al. [81] that ImageNet pretraining does not necessarily provide large performance gains. In addition, the scale of the features may play a role at the effectiveness of ImageNet-based transfer learning (i.e. task 2 images are magnified twice as much as those in task 1); further investigation is needed to better understand this interplay.

### 5.3 Tasks 3–5: microsatellite instability detection

Microsatellite instability (MSI) is an important prognostic clinical biomarker and has generated strong interest in recent years. MSI causes an abundance of DNA mutations and the formation of neoantigens, which activate the immune system, and causes changes in tissue morphology [74, 82, 83]. MSI is a useful clinical biomarker and is an indicator for PD-1/PD-L1 blocking therapies, like pembrolizumab [84–88]. Cercek et al. [89] recently found that their PD-1-blocking therapy led to remission in all 18

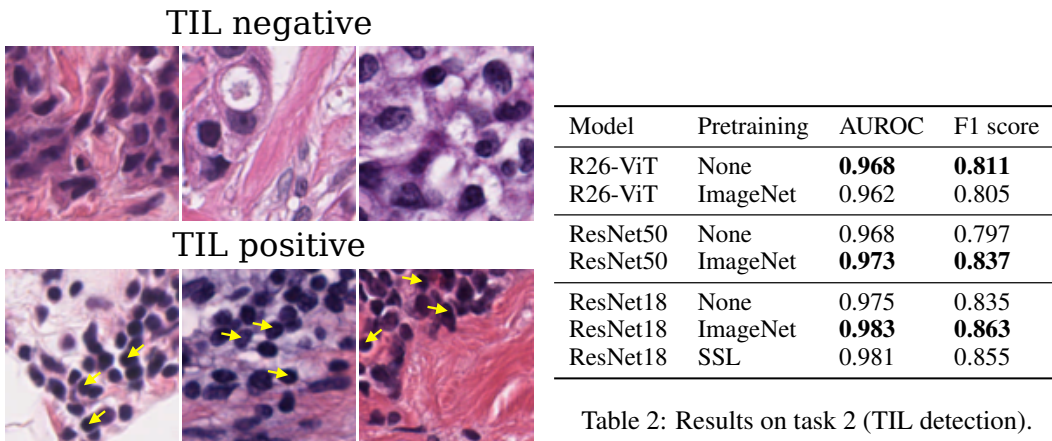


Table 2: Results on task 2 (TIL detection).

Figure 3: Sample images from TILs dataset [55]. The yellow arrows point to examples of TILs.

study participants. If a pathologist suspects an MSI phenotype, the standard of care is to conduct confirmatory molecular testing. Previously, Kather et al. [24] found that they could potentially avoid the time and cost of molecular testing by detecting MSI directly from histopathology. Many similar studies have been conducted [25, 28, 90–94], highlighting the importance of and excitement around MSI. We have included MSI detection in different cancer types and/or tissue preparations as tasks 3–5 because of the strong interest in predicting MSI from histopathology and the clinical relevance of MSI.

**Dataset.** MSI data was curated from [24], which includes images from formalin-fixed, paraffin-embedded samples of colorectal carcinoma (CRC) and stomach adenocarcinoma (STAD) [56] and images from frozen samples of CRC [57]. All images are  $224 \times 224$  pixels at  $0.5 \mu\text{m}/\text{pixel}$  (Figure 4, Table 5 in Appendix). These datasets are publicly available and licensed under Creative Commons Attribution 4.0 International, and all images are anonymized. These datasets are available for immediate download via Zenodo (task 3 [56], task 4 [57], and task 5 [56]).

**Results.** Table 3 summarizes the results. ImageNet-pretrained ResNet50 consistently yielded the best performance across tasks. On the other hand, R26-ViT and ResNet18 yielded inconsistent results with pretraining. In some datasets, the best models were trained from random weight initialization. In other cases, ImageNet or self-supervised learning (SSL) pretraining was superior. The R26-ViT had competitive performance on task 3 (CRC — FFPE) but yielded the worst performance on task 4 (CRC — frozen) and task 5 (STAD). This suggests that the benefit of pretraining is task-specific.

Interestingly, Kather et al. [24] report patient-level AUROCs of 0.77 for CRC (FFPE), 0.84 for CRC (frozen), and 0.81 for STAD. We speculate that our AUROC values are lower because patch-level classification is a more difficult task than patient-level (i.e. whole-slide) classification.

The F1 scores are much lower, indicating poor precision and/or recall. Upon further inspection, there appears to be a wide test-validation gap; the AUROCs on the validation set were much higher (around 0.99). This suggests that the patch-level models are learning spurious correlations within individual patients (across training and validations sets) that do not generalize well to new patients in held-out test data. One strategy to combat this is to ensure that the validation set uses held-out patient data instead of a random split.

#### 5.4 Task 6: precancerous versus benign

Colonoscopies are an important screening test for colorectal carcinoma. Polyps are commonly found during the procedure [95], and these polyps can be benign, precancerous, or cancerous. It is critical to correctly classify a benign polyp from one with cancerous potential because cancerous polyps might indicate need for additional treatment, but distinguishing between these remains challenging [96]. False negatives are unacceptable in this task, and as such, there is significant interest in using deep learning to robustly detect precancerous polyps [97–99]. Due to the clinical importance of detecting precancerous colorectal polyps and the growing interest in applying deep learning to this problem, we elected to use the MHIST dataset [59] for task 6.

**Dataset.** This dataset includes images of hyperplastic polyps and sessile serrated adenomas (Figure 5). Hyperplasia is a benign overgrowth of cells, and an adenoma is a precancerous, low-grade disordered growth of cells. MHIST consists of 3,152 images colorectal polyps. The images were

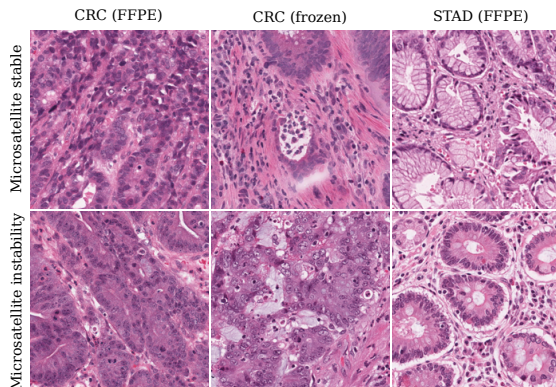


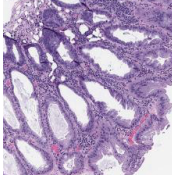
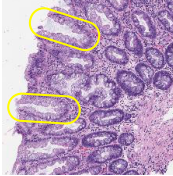
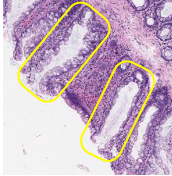
Figure 4: Sample images from MSI datasets. Histologic features of MSI include poorly differentiated cells, signet ring cells, mucinous histology, cribriforming, and lymphocytic infiltrate [83]. FFPE and frozen are two different types of tissue preparations.

Model	Pretraining	Task 3 (CRC — FFPE)		Task 4 (CRC — frozen)		Task 5 (STAD — FFPE)	
		AUROC	F1	AUROC	F1	AUROC	F1
R26-ViT	None	<b>0.710</b>	<b>0.476</b>	0.653	<b>0.383</b>	<b>0.660</b>	<b>0.429</b>
R26-ViT	ImageNet	0.657	0.408	<b>0.704</b>	0.367	0.658	0.396
ResNet50	None	0.480	0.351	0.626	0.326	0.576	0.370
ResNet50	ImageNet	<b>0.710</b>	<b>0.507</b>	<b>0.736</b>	<b>0.475</b>	<b>0.747</b>	<b>0.513</b>
ResNet18	None	0.693	<b>0.468</b>	0.679	<b>0.420</b>	0.685	0.425
ResNet18	ImageNet	<b>0.708</b>	0.454	<b>0.688</b>	0.397	0.705	<b>0.479</b>
ResNet18	SSL	0.681	0.456	0.679	0.396	<b>0.717</b>	0.465

Table 3: Tasks 3–5 results. MSI detection in colorectal carcinoma (CRC) and stomach adenocarcinoma (STAD) with FFPE or frozen preparations.

labeled as hyperplastic or adenomas by seven pathologists, and a binary classification is made by majority vote. All images are  $224 \times 224$  pixels at 8x magnification and are deidentified. The MHIST dataset is the smallest dataset included in ChampKit (Table 5 in Appendix), and this provides a useful test of how well different models and pretraining strategies cope with a small data regime. To access the dataset, one must complete an online form. The user should then receive an automated email with a link to download the dataset. Once the dataset is downloaded, ChampKit can be used to prepare the dataset and train and evaluate models on the data.

**Results.** Unlike in the previous tasks, pretraining dramatically improves performance across all models (Table 4), consistent with the original MHIST publication [59]. Resnet18 performed best overall, consistent with [30]. It was difficult to train models from randomly initialized weights, and the low AUROC and F1 scores reflect this. The R26-ViT in particular achieved an F1 score of 0.00, suggesting that it is especially challenging to train an R26-ViT from scratch on small histopathology datasets. We speculate that pretraining was especially important here because of the small dataset size. Pretraining might provide useful initializations for other small datasets.

Hyperplasia (benign)			
			
Sessile Serrated Adenoma (precancerous)			
			

Model	Pretraining	AUROC	F1 score
R26-ViT	None	0.680	0.000
R26-ViT	ImageNet	<b>0.882</b>	<b>0.784</b>
ResNet50	None	0.672	0.210
ResNet50	ImageNet	<b>0.884</b>	<b>0.741</b>
ResNet18	None	0.665	0.282
ResNet18	ImageNet	<b>0.919</b>	<b>0.804</b>
ResNet18	SSL	0.911	0.768

Table 4: Results on task 6 (precancerous versus benign).

Figure 5: Sample images from MHIST dataset [59]. Colonic crypts are outlined in yellow. Please note the difference in appearance between hyperplasia and adenoma.

## 6 Conclusion

Here we introduce ChampKit, a reproducible benchmarking toolkit for patch-based image classification in histopathology. We use ChampKit to provide baseline results for multiple models on six histopathology datasets. We found that transfer learning can improve classification performance, but this is not consistent across tasks. It remains unclear whether the scale of the histopathology features (i.e., magnification) plays a role in being amenable to transfer learning based on models pretrained on natural images. ChampKit enables the systematic evaluation of transfer learning on patch-based image classification, and we hope that it will greatly advance the knowledge of transfer learning and modeling innovations in histopathology.

In this study, the baseline comparisons were limited to three networks with different pretrained weights. Thus, strong claims of modeling choices cannot be drawn from such a small scale study. Nevertheless, ChampKit uses `timm` to enable easy access to hundreds of other models with different pretrained weights that were not explored here. Hence, it should enable more systematic studies to investigate how model choices, such as small architectures vs large architectures, CNNs vs transformers, transfer learning with pretraining on ImageNet vs self-supervised pretraining vs random initialization, or other modeling choices. In addition, one training run is shown per model here. While these runs are fully reproducible when using the same random number seed, the distribution of training results using multiple seeds can help evaluate the robustness of model performance. Moreover, other patch-level histopathology tasks, including tumor subtype and grade classification, should also be added to expand the benchmark to other popular deep learning applications.

In summary, we hope that ChampKit accelerates research in deep learning and histopathology towards a future in clinical practice.

## Acknowledgments and Disclosure of Funding

We gratefully acknowledge support from National Cancer Institute grants U24CA215109 and UH3CA225021. PKK was supported in part by funding from the Simons Center for Quantitative Biology at Cold Spring Harbor Laboratory. JRK was also supported by National Institutes of Health grant T32GM008444 (NIGMS). JRK would also like to acknowledge the support of the Medical Scientist Training Program at Stony Brook University. The results shown here are in part based upon data generated by the TCGA Research Network: <https://www.cancer.gov/tcga>. We thank Shushan Toneyan for going through the source code and reproducing parts of this manuscript. Finally, we would like to thank Satrajit S. Ghosh for help in naming this project.

## References

- [1] Ross Wightman. Pytorch image models. <https://github.com/rwightman/pytorch-image-models>, 2019.
- [2] Lukas Biewald. Experiment tracking with weights and biases, 2020. URL <https://www.wandb.com/>. Software available from wandb.com.
- [3] Jeroen Van der Laak, Geert Litjens, and Francesco Ciompi. Deep learning in histopathology: the path to the clinic. *Nature medicine*, 27(5):775–784, 2021.
- [4] Sugata Banerji and Sushmita Mitra. Deep learning in histopathology: A review. *Wiley Interdisciplinary Reviews: Data Mining and Knowledge Discovery*, 12(1):e1439, 2022.
- [5] Ahmed S Sultan, Mohamed A Elgharib, Tiffany Tavares, Maryam Jessri, and John R Basile. The use of artificial intelligence, machine learning and deep learning in oncologic histopathology. *Journal of Oral Pathology & Medicine*, 49(9):849–856, 2020.
- [6] Oscar Jimenez-del Toro, Sebastian Otálora, Mats Andersson, Kristian Eurén, Martin Hedlund, Mikael Rousson, Henning Müller, and Manfredo Atzori. Analysis of histopathology images: From traditional machine learning to deep learning. In *Biomedical Texture Analysis*, pages 281–314. Elsevier, 2017.
- [7] Chetan L Srinidhi, Ozan Ciga, and Anne L Martel. Deep neural network models for computational histopathology: A survey. *Medical Image Analysis*, 67:101813, 2021.

- [8] Shujian Deng, Xin Zhang, Wen Yan, Eric I Chang, Yubo Fan, Maode Lai, Yan Xu, et al. Deep learning in digital pathology image analysis: a survey. *Frontiers of medicine*, 14(4):470–487, 2020.
- [9] Azam Hamidinekoo, Erika Denton, Andrik Rampun, Kate Honnor, and Reyer Zwiggelaar. Deep learning in mammography and breast histology, an overview and future trends. *Medical image analysis*, 47:45–67, 2018.
- [10] Nicolas Coudray, Paolo Santiago Ocampo, Theodore Sakellaropoulos, Navneet Narula, Matija Snuderl, David Fenyö, Andre L Moreira, Narges Razavian, and Aristotelis Tsirigos. Classification and mutation prediction from non-small cell lung cancer histopathology images using deep learning. *Nature medicine*, 24(10):1559–1567, 2018.
- [11] Yun Liu, Krishna Gadepalli, Mohammad Norouzi, George E Dahl, Timo Kohlberger, Aleksey Boyko, Subhashini Venugopalan, Aleksei Timofeev, Philip Q Nelson, Greg S Corrado, et al. Detecting cancer metastases on gigapixel pathology images. *arXiv preprint arXiv:1703.02442*, 2017.
- [12] Dayong Wang, Aditya Khosla, Rishab Gargeya, Humayun Irshad, and Andrew H Beck. Deep learning for identifying metastatic breast cancer. *arXiv preprint arXiv:1606.05718*, 2016.
- [13] Byungjae Lee and Kyunghyun Paeng. A robust and effective approach towards accurate metastasis detection and pn-stage classification in breast cancer. In *International conference on medical image computing and computer-assisted intervention*, pages 841–850. Springer, 2018.
- [14] Ruqayya Awan, Navid Alemi Koohbanani, Muhammad Shaban, Anna Lisowska, and Nasir Rajpoot. Context-aware learning using transferable features for classification of breast cancer histology images. In *International conference image analysis and recognition*, pages 788–795. Springer, 2018.
- [15] Osamu Iizuka, Fahdi Kanavati, Kei Kato, Michael Rambeau, Koji Arihiro, and Masayuki Tsuneki. Deep learning models for histopathological classification of gastric and colonic epithelial tumours. *Scientific reports*, 10(1):1–11, 2020.
- [16] Scotty Kwok. Multiclass classification of breast cancer in whole-slide images. In *International conference image analysis and recognition*, pages 931–940. Springer, 2018.
- [17] Joel Saltz, Rajarsi Gupta, Le Hou, Tahsin Kurc, Pankaj Singh, Vu Nguyen, Dimitris Samaras, Kenneth R Shroyer, Tianhao Zhao, Rebecca Batiste, and John Van Arnam. Spatial organization and molecular correlation of tumor-infiltrating lymphocytes using deep learning on pathology images. *Cell Reports*, 23(1):181–193, 2018.
- [18] Shahira Abousamra, Rajarsi Gupta, Le Hou, Rebecca Batiste, Tianhao Zhao, Anand Shankar, Arvind Rao, Chao Chen, Dimitris Samaras, Tahsin Kurc, and Joel Saltz. Deep learning-based mapping of tumor infiltrating lymphocytes in whole slide images of 23 types of cancer. *Frontiers in Oncology*, 11, 2022. ISSN 2234-943X. doi: 10.3389/fonc.2021.806603. URL <https://doi.org/10.3389/fonc.2021.806603>.
- [19] Zixiao Lu, Siwen Xu, Wei Shao, Yi Wu, Jie Zhang, Zhi Han, Qianjin Feng, and Kun Huang. Deep-learning-based characterization of tumor-infiltrating lymphocytes in breast cancers from histopathology images and multiomics data. *JCO clinical cancer informatics*, 4:480–490, 2020.
- [20] Nina Linder, Jenny C Taylor, Richard Colling, Robert Pell, Edward Alveyn, Johnson Joseph, Andrew Protheroe, Mikael Lundin, Johan Lundin, and Clare Verrill. Deep learning for detecting tumour-infiltrating lymphocytes in testicular germ cell tumours. *Journal of clinical pathology*, 72(2):157–164, 2019.
- [21] André LS Meirelles, Tahsin Kurc, Joel Saltz, and George Teodoro. Effective active learning in digital pathology: A case study in tumor infiltrating lymphocytes. *Computer Methods and Programs in Biomedicine*, 220:106828, 2022.
- [22] Ujjwal Baid, Sarthak Pati, Tahsin M Kurc, Rajarsi Gupta, Erich Bremer, Shahira Abousamra, Siddhesh P Thakur, Joel H Saltz, and Spyridon Bakas. Federated learning for the classification of tumor infiltrating lymphocytes. *arXiv preprint arXiv:2203.16622*, 2022.

- [23] Mohamed Amgad, Elisabeth Specht Stovgaard, Eva Balslev, Jeppe Thagaard, Weijie Chen, Sarah Dudgeon, Ashish Sharma, Jennifer K Kerner, Carsten Denkert, Yinyin Yuan, et al. Report on computational assessment of tumor infiltrating lymphocytes from the international immuno-oncology biomarker working group. *NPJ breast cancer*, 6(1):1–13, 2020.
- [24] Jakob Nikolas Kather, Alexander T Pearson, Niels Halama, Dirk Jäger, Jeremias Krause, Sven H Loosen, Alexander Marx, Peter Boor, Frank Tacke, Ulf Peter Neumann, et al. Deep learning can predict microsatellite instability directly from histology in gastrointestinal cancer. *Nature Medicine*, 25(7):1054–1056, Jul 2019. ISSN 1546-170X. doi: 10.1038/s41591-019-0462-y. URL <https://doi.org/10.1038/s41591-019-0462-y>.
- [25] Amelie Echle, Heike Irmgard Grabsch, Philip Quirke, Piet A van den Brandt, Nicholas P West, Gordon GA Hutchins, Lara R Heij, Xiuxiang Tan, Susan D Richman, Jeremias Krause, et al. Clinical-grade detection of microsatellite instability in colorectal tumors by deep learning. *Gastroenterology*, 159(4):1406–1416, 2020.
- [26] Hannah Sophie Muti, Lara Rosaline Heij, Gisela Keller, Meike Kohlruss, Rupert Langer, Bastian Dislich, Jae-Ho Cheong, Young-Woo Kim, Hyunki Kim, Myeong-Cherl Kook, et al. Development and validation of deep learning classifiers to detect epstein-barr virus and microsatellite instability status in gastric cancer: a retrospective multicentre cohort study. *The Lancet Digital Health*, 3(10):e654–e664, 2021.
- [27] Amelie Echle, Narmin Ghaffari Laleh, Peter L Schrammen, Nicholas P West, Christian Trautwein, Titus J Brinker, Stephen B Gruber, Roman D Buelow, Peter Boor, Heike I Grabsch, et al. Deep learning for the detection of microsatellite instability from histology images in colorectal cancer: a systematic literature review. *ImmunoInformatics*, page 100008, 2021.
- [28] Rui Cao, Fan Yang, Si-Cong Ma, Li Liu, Yu Zhao, Yan Li, De-Hua Wu, Tongxin Wang, Wei-Jia Lu, Wei-Jing Cai, et al. Development and interpretation of a pathomics-based model for the prediction of microsatellite instability in colorectal cancer. *Theranostics*, 10(24):11080, 2020.
- [29] Olga Russakovsky, Jia Deng, Hao Su, Jonathan Krause, Sanjeev Satheesh, Sean Ma, Zhiheng Huang, Andrej Karpathy, Aditya Khosla, Michael Bernstein, Alexander C. Berg, and Li Fei-Fei. ImageNet Large Scale Visual Recognition Challenge. *International Journal of Computer Vision (IJCV)*, 115(3):211–252, 2015. doi: 10.1007/s11263-015-0816-y.
- [30] Yash Sharmay, Lubaina Ehsany, Sana Syed, and Donald E Brown. Histotransfer: Understanding transfer learning for histopathology. In *2021 IEEE EMBS International Conference on Biomedical and Health Informatics (BHI)*, pages 1–4. IEEE, 2021.
- [31] Maximilian Springenberg, Annika Frommholz, Markus Wenzel, Eva Weicken, Jackie Ma, and Nils Strodthoff. From cnns to vision transformers—a comprehensive evaluation of deep learning models for histopathology. *arXiv preprint arXiv:2204.05044*, 2022.
- [32] Sara Hosseinzadeh Kassani, Peyman Hosseinzadeh Kassani, Michal J Wesolowski, Kevin A Schneider, and Ralph Deters. Classification of histopathological biopsy images using ensemble of deep learning networks. *arXiv preprint arXiv:1909.11870*, 2019.
- [33] Ozan Ciga, Tony Xu, and Anne Louise Martel. Self supervised contrastive learning for digital histopathology. *Machine Learning with Applications*, 7:100198, 2022. ISSN 2666-8270. doi: <https://doi.org/10.1016/j.mlwa.2021.100198>. URL <https://www.sciencedirect.com/science/article/pii/S2666827021000992>.
- [34] Xiyue Wang, Sen Yang, Jun Zhang, Minghui Wang, Jing Zhang, Junzhou Huang, Wei Yang, and Xiao Han. Transpath: Transformer-based self-supervised learning for histopathological image classification. In *International Conference on Medical Image Computing and Computer-Assisted Intervention*, pages 186–195. Springer, 2021.
- [35] Mingyu Chen, Bin Zhang, Win Topatana, Jiasheng Cao, Hepan Zhu, Sarun Juengpanich, Qijiang Mao, Hong Yu, and Xiujun Cai. Classification and mutation prediction based on histopathology h&e images in liver cancer using deep learning. *NPJ precision oncology*, 4(1):1–7, 2020.

- [36] Neslihan Bayramoglu, Juho Kannala, and Janne Heikkilä. Deep learning for magnification independent breast cancer histopathology image classification. In *2016 23rd International conference on pattern recognition (ICPR)*, pages 2440–2445. IEEE, 2016.
- [37] Zabit Hameed, Sofia Zahia, Begonya Garcia-Zapirain, José Javier Aguirre, and Ana María Vane-gas. Breast cancer histopathology image classification using an ensemble of deep learning models. *Sensors*, 20(16):4373, 2020.
- [38] Adam Paszke, Sam Gross, Francisco Massa, Adam Lerer, James Bradbury, Gregory Chanan, Trevor Killeen, Zeming Lin, Natalia Gimelshein, Luca Antiga, Alban Desmaison, Andreas Kopf, Edward Yang, Zachary DeVito, Martin Raison, Alykhan Tejani, Sasank Chilamkurthy, Benoit Steiner, Lu Fang, Junjie Bai, and Soumith Chintala. Pytorch: An imperative style, high-performance deep learning library. In H. Wallach, H. Larochelle, A. Beygelzimer, F. d'Alché-Buc, E. Fox, and R. Garnett, editors, *Advances in Neural Information Processing Systems 32*, pages 8024–8035. Curran Associates, Inc., 2019. URL <http://papers.neurips.cc/paper/9015-pytorch-an-imperative-style-high-performance-deep-learning-library.pdf>.
- [39] Martín Abadi, Ashish Agarwal, Paul Barham, Eugene Brevdo, Zhifeng Chen, Craig Citro, Greg S. Corrado, Andy Davis, Jeffrey Dean, Matthieu Devin, Sanjay Ghemawat, Ian Goodfellow, Andrew Harp, Geoffrey Irving, Michael Isard, Yangqing Jia, Rafal Jozefowicz, Lukasz Kaiser, Manjunath Kudlur, Josh Levenberg, Dandelion Mané, Rajat Monga, Sherry Moore, Derek Murray, Chris Olah, Mike Schuster, Jonathon Shlens, Benoit Steiner, Ilya Sutskever, Kunal Talwar, Paul Tucker, Vincent Vanhoucke, Vijay Vasudevan, Fernanda Viégas, Oriol Vinyals, Pete Warden, Martin Wattenberg, Martin Wicke, Yuan Yu, and Xiaoqiang Zheng. TensorFlow: Large-scale machine learning on heterogeneous systems, 2015. URL <https://www.tensorflow.org/>. Software available from tensorflow.org.
- [40] Thomas Wolf, Lysandre Debut, Victor Sanh, Julien Chaumond, Clement Delangue, Anthony Moi, Péric Cistac, Clara Ma, Yacine Jernite, Julien Plu, Canwen Xu, Teven Le Scao, Sylvain Gugger, Mariama Drame, Quentin Lhoest, and Alexander M. Rush. Transformers: State-of-the-Art Natural Language Processing. In *Proceedings of the 2020 Conference on Empirical Methods in Natural Language Processing: System Demonstrations*, pages 38–45. Association for Computational Linguistics, 10 2020. URL <https://www.aclweb.org/anthology/2020.emnlp-demos.6>.
- [41] François Chollet et al. Keras. <https://keras.io>, 2015.
- [42] Magdy Abd-Elghany Zeid, Khaled El-Bahnasy, and SE Abo-Youssef. Multiclass colorectal cancer histology images classification using vision transformers. In *2021 Tenth International Conference on Intelligent Computing and Information Systems (ICICIS)*, pages 224–230. IEEE, 2021.
- [43] Haoyuan Chen, Chen Li, Ge Wang, Xiaoyan Li, Md Rahaman, Hongzan Sun, Weiming Hu, Yixin Li, Wanli Liu, Changhao Sun, et al. Gashis-transformer: A multi-scale visual transformer approach for gastric histopathological image detection. *Pattern Recognition*, page 108827, 2022.
- [44] Luca Deiningner, Bernhard Stimpel, Anil Yuce, Samaneh Abbasi-Sureshjani, Simon Schönenberger, Paolo Ocampo, Konstanty Korski, and Fabien Gaire. A comparative study between vision transformers and cnns in digital pathology. *arXiv preprint arXiv:2206.00389*, 2022.
- [45] Narmin Ghaffari Laleh, Hannah Sophie Muti, Chiara Maria Lavinia Loeffler, Amelie Echle, Oliver Lester Saldanha, Faisal Mahmood, Ming Y Lu, Christian Trautwein, Rupert Langer, Bastian Dislich, Roman D Buelow, Heike Irmgard Grabsch, Hermann Brenner, Jenny Chang-Claude, Elizabeth Alwers, Titus J Brinker, Firas Khader, Daniel Truhn, Nadine T Gaisa, Peter Boor, Michael Hoffmeister, Volkmar Schulz, and Jakob Nikolas Kather. Benchmarking weakly-supervised deep learning pipelines for whole slide classification in computational pathology. *Medical image analysis*, 79:102474, 2022.
- [46] Kaiming He, Xiangyu Zhang, Shaoqing Ren, and Jian Sun. Deep residual learning for image recognition. In *Proceedings of the IEEE conference on computer vision and pattern recognition*, pages 770–778, 2016.

- [47] Gao Huang, Zhuang Liu, Laurens Van Der Maaten, and Kilian Q Weinberger. Densely connected convolutional networks. In *Proceedings of the IEEE conference on computer vision and pattern recognition*, pages 4700–4708, 2017.
- [48] Mingxing Tan and Quoc Le. Efficientnet: Rethinking model scaling for convolutional neural networks. In *International conference on machine learning*, pages 6105–6114. PMLR, 2019.
- [49] Babak Ehteshami Bejnordi, Mitko Veta, Paul Johannes Van Diest, Bram Van Ginneken, Nico Karssemeijer, Geert Litjens, Jeroen AWM Van Der Laak, Meyke Hermsen, Quirine F Manson, Maschenka Balkenhol, et al. Diagnostic assessment of deep learning algorithms for detection of lymph node metastases in women with breast cancer. *Jama*, 318(22):2199–2210, 2017.
- [50] Hugo Touvron, Matthieu Cord, Matthijs Douze, Francisco Massa, Alexandre Sablayrolles, and Herve Jegou. Training data-efficient image transformers & distillation through attention. In *International Conference on Machine Learning*, volume 139, pages 10347–10357, July 2021.
- [51] Jakob Nikolas Kather, Niels Halama, and Alexander Marx. 100,000 histological images of human colorectal cancer and healthy tissue, April 2018. URL <https://doi.org/10.5281/zenodo.1214456>.
- [52] Karen Simonyan and Andrew Zisserman. Very deep convolutional networks for large-scale image recognition. *arXiv preprint arXiv:1409.1556*, 2014.
- [53] Andrew G Howard, Menglong Zhu, Bo Chen, Dmitry Kalenichenko, Weijun Wang, Tobias Weyand, Marco Andreetto, and Hartwig Adam. Mobilenets: Efficient convolutional neural networks for mobile vision applications. *arXiv preprint arXiv:1704.04861*, 2017.
- [54] Ozan Ciga. Native pytorch weights (trained with 400 thousand images). <https://github.com/ozanciga/self-supervised-histopathology/releases/tag/nativetenpercent>, 2022.
- [55] Jakub R Kaczmarzyk, Shahira Abousamra, Tahsin Kurc, Rajarsi Gupta, and Joel Saltz. Dataset for tumor infiltrating lymphocyte classification (304,097 images from TCGA), June 2022. URL <https://doi.org/10.5281/zenodo.6604094>.
- [56] Jakob Nikolas Kather. Histological images for MSI vs. MSS classification in gastrointestinal cancer, FFPE samples, February 2019. URL <https://doi.org/10.5281/zenodo.2530835>.
- [57] Jakob Nikolas Kather. Histological images for MSI vs. MSS classification in gastrointestinal cancer, snap-frozen samples, February 2019. URL <https://doi.org/10.5281/zenodo.2532612>.
- [58] Bastiaan S Veeling, Jasper Linmans, Jim Winkens, Taco Cohen, and Max Welling. Rotation equivariant cnns for digital pathology. In *International Conference on Medical image computing and computer-assisted intervention*, pages 210–218. Springer, 2018. URL [https://doi.org/10.1007/978-3-030-00934-2\\_24](https://doi.org/10.1007/978-3-030-00934-2_24).
- [59] Jerry Wei, Arief Suriawinata, Bing Ren, Xiaoying Liu, Mikhail Lisovsky, Louis Vaickus, Charles Brown, Michael Baker, Naofumi Tomita, Lorenzo Torresani, Jason Wei, and Saeed Hassanpour. A petri dish for histopathology image analysis. In *International Conference on Artificial Intelligence in Medicine*, pages 11–24. Springer, 2021. URL [https://doi.org/10.1007/978-3-030-77211-6\\_2](https://doi.org/10.1007/978-3-030-77211-6_2).
- [60] Alexey Dosovitskiy, Lucas Beyer, Alexander Kolesnikov, Dirk Weissenborn, Xiaohua Zhai, Thomas Unterthiner, Mostafa Dehghani, Matthias Minderer, Georg Heigold, Sylvain Gelly, et al. An image is worth 16x16 words: Transformers for image recognition at scale. *arXiv preprint arXiv:2010.11929*, 2020.
- [61] Ilya Loshchilov and Frank Hutter. Decoupled weight decay regularization. *arXiv preprint arXiv:1711.05101*, 2017.
- [62] Gao Huang, Yu Sun, Zhuang Liu, Daniel Sedra, and Kilian Q. Weinberger. Deep networks with stochastic depth. In Bastian Leibe, Jiri Matas, Nicu Sebe, and Max Welling, editors, *Computer Vision – ECCV 2016*, pages 646–661, Cham, 2016. Springer International Publishing. ISBN 978-3-319-46493-0. URL [https://doi.org/10.1007/978-3-319-46493-0\\_39](https://doi.org/10.1007/978-3-319-46493-0_39).

- [63] Christian Szegedy, Vincent Vanhoucke, Sergey Ioffe, Jon Shlens, and Zbigniew Wojna. Rethinking the inception architecture for computer vision. In *Proceedings of the IEEE conference on computer vision and pattern recognition*, pages 2818–2826, 2016.
- [64] Ekin D Cubuk, Barret Zoph, Jonathon Shlens, and Quoc V Le. Randaugment: Practical automated data augmentation with a reduced search space. In *Proceedings of the IEEE/CVF Conference on Computer Vision and Pattern Recognition Workshops*, pages 702–703, 2020.
- [65] Zhun Zhong, Liang Zheng, Guoliang Kang, Shaozi Li, and Yi Yang. Random erasing data augmentation. In *Proceedings of the AAAI Conference on Artificial Intelligence (AAAI)*, 2020.
- [66] Nicki Skafté Detlefsen, Jiri Borovec, Justus Schock, Ananya Harsh, Teddy Koker, Luca Di Liello, Daniel Stancl, Changsheng Quan, Maxim Grechkin, and William Falcon. TorchMetrics - Measuring Reproducibility in PyTorch, 2 2022. URL <https://github.com/PyTorchLightning/metrics>.
- [67] Yun Liu, Timo Kohlberger, Mohammad Norouzi, George E Dahl, Jenny L Smith, Arash Mohtashamian, Niels Olson, Lily H Peng, Jason D Hipp, and Martin C Stumpe. Artificial intelligence–based breast cancer nodal metastasis detection: Insights into the black box for pathologists. *Archives of Pathology & Laboratory Medicine*, 143(7):859–868, 2019.
- [68] College of American Pathologists. Protocol for the examination of resection specimens from patients with invasive carcinoma of the breast, March 2022. URL [https://documents.cap.org/protocols/Breast.Invasive\\_4.6.0.0.REL\\_CAPCP.pdf](https://documents.cap.org/protocols/Breast.Invasive_4.6.0.0.REL_CAPCP.pdf).
- [69] Bastiaan S Veeling, Jasper Linmans, Jim Winkens, Taco Cohen, and Max Welling. Rotation Equivariant CNNs for Digital Pathology, September 2018. URL <https://zenodo.org/record/2546921>.
- [70] Gregory E Idos, Janet Kwok, Nirupama Bonthala, Lynn Kysh, Stephen B Gruber, and Chenxu Qu. The prognostic implications of tumor infiltrating lymphocytes in colorectal cancer: a systematic review and meta-analysis. *Scientific Reports*, 10(1):1–14, 2020.
- [71] Sterre T Paijens, Annegé Vledder, Marco de Bruyn, and Hans W Nijman. Tumor-infiltrating lymphocytes in the immunotherapy era. *Cellular & Molecular Immunology*, 18(4):842–859, 2021.
- [72] Franck Pagès, Bernhard Mlecnik, Florence Marliot, Gabriela Bindea, Fang-Shu Ou, Carlo Bifulco, Alessandro Lugli, Inti Zlobec, Tilman T Rau, Martin D Berger, et al. International validation of the consensus immunoscore for the classification of colon cancer: a prognostic and accuracy study. *The Lancet*, 391(10135):2128–2139, 2018.
- [73] Muhammad Shaban, Syed Ali Khurram, Muhammad Moazam Fraz, Najah Alsubaie, Iqra Masood, Sajid Mushtaq, Mariam Hassan, Asif Loya, and Nasir M Rajpoot. A novel digital score for abundance of tumour infiltrating lymphocytes predicts disease free survival in oral squamous cell carcinoma. *Scientific reports*, 9(1):1–13, 2019.
- [74] Vinay Kumar, Abul K. Abbas, and Jon C. Aster. *Robbins Basic Pathology*. Elsevier, Philadelphia, 2017.
- [75] Danielle J. Fassler, Luke A. Torre-Healy, Rajarsi Gupta, Alina M. Hamilton, Soma Kobayashi, Sarah C. Van Alsten, Yuwei Zhang, Tahsin Kurc, Richard A. Moffitt, Melissa A. Troester, Katherine A. Hoadley, and Joel Saltz. Spatial characterization of tumor-infiltrating lymphocytes and breast cancer progression. *Cancers*, 14(9):2148, Apr 2022. ISSN 2072-6694. doi: 10.3390/cancers14092148. URL <http://dx.doi.org/10.3390/cancers14092148>.
- [76] Roberto Salgado, Carsten Denkert, S Demaria, N Sirtaine, F Klauschen, Giancarlo Pruneri, S Wienert, Gert Van den Eynden, Frederick L Baehner, Frederique Pénault-Llorca, et al. The evaluation of tumor-infiltrating lymphocytes (tils) in breast cancer: recommendations by an international tils working group 2014. *Annals of Oncology*, 26(2):259–271, 2015.

- [77] Han Le, Rajarsi Gupta, Le Hou, Shahira Abousamra, Danielle Fassler, Luke Torre-Healy, Richard A. Moffitt, Tahsin Kurc, Dimitris Samaras, Rebecca Batiste, Tianhao Zhao, Arvind Rao, Alison L. Van Dyke, Ashish Sharma, Erich Bremer, Jonas S. Almeida, and Joel Saltz. Utilizing automated breast cancer detection to identify spatial distributions of tumor-infiltrating lymphocytes in invasive breast cancer. *The American journal of pathology*, 190(7):1491–1504, 2020.
- [78] Xiaoxuan Zhang, Xiongfeng Zhu, Kai Tang, Yinghua Zhao, Zixiao Lu, and Qianjin Feng. Ddtnet: A dense dual-task network for tumor-infiltrating lymphocyte detection and segmentation in histopathological images of breast cancer. *Medical Image Analysis*, 78:102415, 2022. ISSN 1361-8415. doi: <https://doi.org/10.1016/j.media.2022.102415>. URL <https://www.sciencedirect.com/science/article/pii/S1361841522000676>.
- [79] Katherine A Hoadley, Christina Yau, Toshinori Hinoue, Denise M Wolf, Alexander J Lazar, Esther Drill, Ronglai Shen, Alison M Taylor, Andrew D Cherniack, Vésteinn Thorsson, et al. Cell-of-origin patterns dominate the molecular classification of 10,000 tumors from 33 types of cancer. *Cell*, 173(2):291–304, 2018.
- [80] Simon Kornblith, Jonathon Shlens, and Quoc V Le. Do better imagenet models transfer better? In *Proceedings of the IEEE/CVF conference on computer vision and pattern recognition*, pages 2661–2671, 2019.
- [81] Maithra Raghu, Chiyuan Zhang, Jon Kleinberg, and Samy Bengio. Transfusion: Understanding transfer learning for medical imaging. *Advances in neural information processing systems*, 32, 2019.
- [82] Giovanni Germano, Simona Lamba, Giuseppe Rospo, Ludovic Barault, Alessandro Magrì, Federica Maione, Mariangela Russo, Giovanni Crisafulli, Alice Bartolini, Giulia Lerda, et al. Inactivation of dna repair triggers neoantigen generation and impairs tumour growth. *Nature*, 552(7683):116–120, 2017.
- [83] Julian Alexander, Toshiaki Watanabe, Tsung-Teh Wu, Asif Rashid, Shuan Li, and Stanley R Hamilton. Histopathological identification of colon cancer with microsatellite instability. *The American journal of pathology*, 158(2):527–535, 2001.
- [84] Sandra J Casak, Leigh Marcus, Lola Fashoyin-Aje, Sirisha L Mushti, Joyce Cheng, Yuan-Li Shen, William F Pierce, Leah Her, Kirsten B Goldberg, Marc R Theoret, et al. Fda approval summary: Pembrolizumab for the first-line treatment of patients with msi-h/dmmr advanced unresectable or metastatic colorectal carcinoma. *Clinical Cancer Research*, 27(17):4680–4684, 2021.
- [85] David M O’Malley, Giovanni Mendonca Bariani, Philippe A Cassier, Aurelien Marabelle, Aaron R Hansen, Ana De Jesus Acosta, Wilson H Miller, Tamar Safra, Antoine Italiano, Linda Mileshkin, et al. Pembrolizumab in patients with microsatellite instability–high advanced endometrial cancer: results from the keynote-158 study. *Journal of Clinical Oncology*, 40(7):752–761, 2022.
- [86] C Luchini, F Bibeau, MJL Ligtenberg, N Singh, A Nottegar, T Bosse, R Miller, N Riaz, J-Y Douillard, F Andre, et al. Esmo recommendations on microsatellite instability testing for immunotherapy in cancer, and its relationship with pd-1/pd-l1 expression and tumour mutational burden: a systematic review-based approach. *Annals of Oncology*, 30(8):1232–1243, 2019.
- [87] F Pietrantonio, G Randon, M Di Bartolomeo, A Luciani, J Chao, EC Smyth, and F Petrelli. Predictive role of microsatellite instability for pd-1 blockade in patients with advanced gastric cancer: a meta-analysis of randomized clinical trials. *ESMO open*, 6(1):100036, 2021.
- [88] Luis A Diaz, Dung T Le, Takayuki Yoshino, Thierry Andre, Johanna C Bendell, Minori Rosales, S Peter Kang, Bao Lam, and Dirk Jäger. Keynote-177: Phase 3, open-label, randomized study of first-line pembrolizumab (pembro) versus investigator-choice chemotherapy for mismatch repair-deficient (dmmr) or microsatellite instability-high (msi-h) metastatic colorectal carc@inproceedingspmlr-v139-touvron21a, title = Training data-efficient image transformers & distillation through attention, author = Touvron, Hugo and Cord, Matthieu and Douze, Matthijs

and Massa, Francisco and Sablayrolles, Alexandre and Jegou, Herve, booktitle = International Conference on Machine Learning, pages = 10347–10357, year = 2021, volume = 139, month = July inoma (mcrc)., 2018.

- [89] Andrea Cercek, Melissa Lumish, Jenna Sinopoli, Jill Weiss, Jinru Shia, Michelle Lamendola-Essel, Imane H. El Dika, Neil Segal, Marina Shcherba, Ryan Sugarman, Zsofia Stadler, Rona Yaeger, J. Joshua Smith, Benoit Rousseau, Guillem Argiles, Miteshkumar Patel, Avni Desai, Leonard B. Saltz, Maria Widmar, Krishna Iyer, Janie Zhang, Nicole Gianino, Christopher Crane, Paul B. Romesser, Emmanouil P. Pappou, Philip Paty, Julio Garcia-Aguilar, Mithat Gonen, Marc Gollub, Martin R. Weiser, Kurt A. Schalper, and Luis A. Diaz. Pd-1 blockade in mismatch repair-deficient, locally advanced rectal cancer. *New England Journal of Medicine*, 2022. doi: 10.1056/NEJMoa2201445. URL <https://doi.org/10.1056/NEJMoa2201445>.
- [90] Rikiya Yamashita, Jin Long, Teri Longacre, Lan Peng, Gerald Berry, Brock Martin, John Higgins, Daniel L Rubin, and Jeanne Shen. Deep learning model for the prediction of microsatellite instability in colorectal cancer: a diagnostic study. *The Lancet Oncology*, 22(1):132–141, 2021.
- [91] Mark A Jenkins, Shinichi Hayashi, Anne-Marie O’shea, Lawrence J Burgart, Tom C Smyrk, David Shimizu, Paul M Waring, Andrew R Ruskiewicz, Aaron F Pollett, Mark Redston, et al. Pathology features in bethesda guidelines predict colorectal cancer microsatellite instability: a population-based study. *Gastroenterology*, 133(1):48–56, 2007.
- [92] Jinru Shia, Nathan A Ellis, Philip B Paty, Garrett M Nash, Jing Qin, Kenneth Offit, Xin-Min Zhang, Arnold J Markowitz, Khedoudja Nafa, Jose G Guillem, et al. Value of histopathology in predicting microsatellite instability in hereditary nonpolyposis colorectal cancer and sporadic colorectal cancer. *The American journal of surgical pathology*, 27(11):1407–1417, 2003.
- [93] Angela Hyde, Daniel Fontaine, Susan Stuckless, Roger Green, Aaron Pollett, Michelle Simms, Payal Sipahimalani, Patrick Parfrey, and Banfield Youngusband. A histology-based model for predicting microsatellite instability in colorectal cancers. *The American journal of surgical pathology*, 34(12):1820–1829, 2010.
- [94] Mohammad Rizwan Alam, Jamshid Abdul-Ghafar, Kwangil Yim, Nishant Thakur, Sung Hak Lee, Hyun-Jong Jang, Chan Kwon Jung, and Yosep Chong. Recent applications of artificial intelligence from histopathologic image-based prediction of microsatellite instability in solid cancers: A systematic review. *Cancers*, 14(11):2590, 2022.
- [95] Joshua C Obuch, Courtney M Pigott, and Dennis J Ahnen. Sessile serrated polyps: detection, eradication, and prevention of the evil twin. *Current Treatment Options in Gastroenterology*, 13(1):156–170, 2015.
- [96] Diana R Jaravaza and Jonathan M Rigby. Hyperplastic polyp or sessile serrated lesion? the contribution of serial sections to reclassification. *Diagnostic Pathology*, 15(1):1–9, 2020.
- [97] Dan Yoon, Hyoun-Joong Kong, Byeong Soo Kim, Woo Sang Cho, Jung Chan Lee, Minwoo Cho, Min Hyuk Lim, Sun Young Yang, Seon Hee Lim, Jooyoung Lee, et al. Colonoscopic image synthesis with generative adversarial network for enhanced detection of sessile serrated lesions using convolutional neural network. *Scientific Reports*, 12(1):1–12, 2022.
- [98] Jason W Wei, Arief A Suriawinata, Louis J Vaickus, Bing Ren, Xiaoying Liu, Mikhail Lisovsky, Naofumi Tomita, Behnaz Abdollahi, Adam S Kim, Dale C Snover, et al. Evaluation of a deep neural network for automated classification of colorectal polyps on histopathologic slides. *JAMA network open*, 3(4):e203398–e203398, 2020.
- [99] Bruno Korbar, Andrea M Olofson, Allen P Miraflor, Catherine M Nicka, Matthew A Suriawinata, Lorenzo Torresani, Arief A Suriawinata, and Saeed Hassanpour. Deep learning for classification of colorectal polyps on whole-slide images. *Journal of pathology informatics*, 8, 2017.

## A Appendix

Table 5: Dataset sizes.

Dataset	Train		Val		Test	
	Positive	Negative	Positive	Negative	Positive	Negative
PatchCamelyon	131,072	131,072	16,369	16,399	16,377	16,391
TILs	39,206	170,015	5,203	33,398	10,501	45,774
MSI STAD	40,228	40,228	10,057	10,057	27,904	90,104
MSI CRC (FFPE)	37,363	37,363	9,341	9,341	28,335	70,569
MSI CRC (frozen)	24,357	24,358	6,090	6,089	17,675	60,574
MHIST	493	1,247	137	298	360	617